



MODE-II INTERLAMINAR FRACTURE INVESTIGATION OF NOVEL SHAPED GLASS FIBRE COMPOSITES

Mr. Alessandro Cannas*, Dr. Ian Bond*, Dr. Amir Rezai**, Mr. Matteo Lusi***
Advanced Composites Centre for Innovation and Science,
Department of Aerospace Engineering, University of Bristol, Queen's Building,
University Walk, BS8 1TR, Bristol, U.K.

Tel: +44 (0)117 331 7499 Fax: +44 (0)117 927 2771 E-mail: a.cannas@bristol.ac.uk

** BAE Systems, Advanced Technical Centre, P.O. Box 5, Filton, BS34 7QW, Bristol, U.K.

*** University of Bristol, School of Chemistry, Cantocks Close, BS8 1TS, Bristol, U.K.

Keywords: *shaped fibre, matrices and interfaces; damage and fracture; strain energy release rate; microstructure/properties.*

Abstract

A study has been conducted to evaluate the benefits of using novel shaped fibre reinforcement to improve mode-II strain energy release rate of fibre reinforced polymer composites (FRP). Unidirectional and cross-ply laminates were manufactured using shaped and circular glass fibre reinforcement and tested using the end notched flexure (ENF) and end loaded split (ELS) geometries. Before testing, each specimen was pre-cracked using mode-I opening. The circular fibres were manufactured to have the same cross-sectional area as the shaped. The strain energy release rate for both crack initiation ($G_{IICinitiation}$) and propagation ($G_{IICpropagation}$) of all manufactured composites was calculated using Corrected Beam Theory (CBT) based on compliance calibration. Due to differences in resin and fibre volume fractions and fibre geometries, a correction factor was applied to the CBT expression to allow a fairer comparison. Results obtained have shown an increase of both $G_{IICinitiation}$ and $G_{IICpropagation}$ values for composites reinforced with shaped fibres.

1 Introduction

Composite materials are increasingly employed for primary structures in aerospace applications, but their poor through-thickness properties limit a wider use even in many other fields of engineering such as automotive, sport and civil infrastructure. Thus, an understanding of the through-thickness response is paramount for the design of reliable structures and often has a controlling influence on the overall structural strength of the components [1].

The through-thickness failure in FRP structures is often a consequence of delamination.

This common failure mode for composite laminates is characterised by interlaminar propagation of defects which can lead to a significant deterioration in performance [2]. In order to fully characterise interlaminar fracture toughness, it is necessary to study the effect of various proportions of normal and shear stresses at the crack tip, including pure tension (mode-I) and pure shear (mode-II) [3]. In this paper mode-II fracture will be studied via ENF and ELS specimens which are commonly used to evaluate the pure mode-II interlaminar fracture toughness [3]. Despite the lack of a standard to determine the mode-II strain energy release rate (G_{IIC}), an increasing number of publications in the literature [1, 6-27] helps to overcome most of the issues relating to testing configurations such as the selection of a specimen type, loading rig, the selection of the film starter, the selection of a method for data analysis and identifying critical factors affecting the test procedure. Moreover, thanks to a series of recent studies, the American Society for Testing and Materials (ASTM) committee D30 on composite materials has resolved to adopt the end notched flexure (ENF) test as the standard method for determining the mode-II delamination toughness, G_{IIC} , for laminated composites [20]. The ENF has been found to offer a consistent, more stable crack initiation compared to other test geometries [5, 9-11, 12, 14, 16, 20]. However, a stable crack propagation is preferentially obtained using end-loaded-split (ELS) specimens [8-9, 14] for which no ASTM standards are yet available.

Care must be taken during specimen preparation to reduce or avoid fibre pull-out, fibre

breakage, fibre bridging, or resin rich pockets which strongly affect the G_{IIC} strain energy release rate measurement [3]. A non-adhesive film is essential to generate a starter crack and allow propagation at the interface of interest [6]. The film inserts used in ENF and ELS specimens can comprise various materials and thicknesses. For example, PTFE, aluminium, mylar and kapton can all be used with thicknesses varying from 10 μm to 60 μm [3-4, 6-7, 13-14, 23, 28-33]. Thinner insert foils (< 13 μm) reduce the resin rich region ahead of the starter film which can otherwise give rise to G_{IIC} values different from that of the bulk composite. Due to the larger diameter of some types of glass-fibres compared to carbon fibres, thicker inserts might still be suitable for GFRP without significantly affecting G_{IIC} measurements. Some film materials, such as PTFE, are not suitable as inserts for higher curing temperatures matrix materials as they may adhere strongly to the matrix. Release agents applied to the insert foils could disperse into the adjacent matrix during curing and affect the matrix properties. Also some film materials, such as aluminium, tend to crimp or fold during placement or curing [3].

It is advisable to pre-crack the specimens to avoid resin rich pockets and to provide a sharp initial crack for the subsequent mode-II test [9, 32]. Pre-cracks can be introduced by loading the specimen in mode-I or driving a wedge into the specimen. The crack extension should be sufficiently long to bypass any resin rich pocket but short enough to avoid fibre bridging [6, 31].

Following specimen preparation, the test is usually carried out at crosshead rate of 1 mm/min [5, 9, 33-34] and experimental data generated must be processed with an appropriate data reduction method. Various data reduction approaches are used for ENF and ELS tests. They take inspiration from many approaches including Classical Beam Theory (CBT), Timoshenko Beam Theory (TBT), Modified Beam Theory (MBT) or Compliance Calibration (CC) [7]. All theories reported above are based on different hypotheses, and correction factors are commonly applied in order to improve accuracy [4, 6, 9, 16, 29, 33].

Excellent review papers on novel architectures to improve the through-thickness properties of composites have been widely published in the literature [35-40]. A new approach based upon novel cross-section fibres is currently being investigated at the University of Bristol. Results to date suggest that judicious selection of fibre shape could lead to an increase in through -thickness strength as well as

improvements in the fracture toughness of FRP composite materials [32, 41-42].

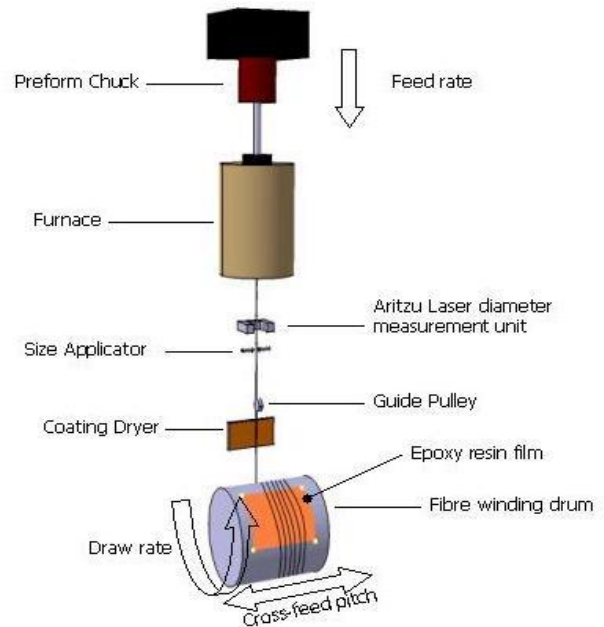


Fig. 1: Schematic of fibre drawing tower facility.

2 Materials

2.1 Fibre and pre-preg manufacture

Solid circular and hollow shaped glass fibres and their pre-pregs have been manufactured at the University of Bristol using a bespoke fibre making tower facility, Figure 1. Depending on the fibre type, either a 6 mm circular or 9.8 mm (4 mm hollowness) hollow shaped borosilicate glass preform (DURANTM by Schott) is attached to the top of the fibre tower. The glass preform is drawn into a single filament, coated with silane coupling agent (3-Amino-propyltrimethoxysilane 95%, Acros Organics) to increase subsequent fibre-matrix bonding strength and wound onto drum covered with a Hexcel 913 epoxy resin film (42 gsm). The rate at which the glass preform is fed into the furnace, the rotational speed of the winding drum and the furnace temperature control the final fibre geometry. A further Hexcel 913 resin film is applied on top of the fibres to form a pre-impregnated tape which is then subject to a full atmospheric vacuum for 45 min at 80°C to facilitate fibre impregnation.

2.2 Sample preparation

In accordance with AECMA standards [1], ESIS TC 4 Meeting [34] and Davidson *et al* [7], composite panels for each reinforcement and geometry were manufactured using a combination of

MODE-II INTERLAMINAR FRACTURE INVESTIGATION OF NOVEL SHAPED GLASS FIBRE COMPOSITES

commercial Hexcel E-glass/913 epoxy and in-house manufactured glass fibre/Hexcel 913 epoxy pre-impregnated tapes. Plates of 230 mm x 230 mm x 6.4 mm (ENF) and 210 mm x 230 mm x 3 mm (ELS) were prepared with stacking sequences shown in Table 1. A 10 μ m thickness PTFE starter film was incorporated to ensure correct crack initiation along the interface of interest in both unidirectional and cross-ply ($0^\circ/90^\circ$) panels. Standard vacuum bagging procedures were used and the panels were processed in an autoclave according to manufacturers recommendations at 7 bars (100 psi) and 1 hour dwell at 120° C for 1 hour but with a preceding of 90 °C dwell for 30 min (recommended for parts in excess of 3 mm thickness). The heating rate was 2 °C min⁻¹ which is within the manufacturer's recommended range. After the curing process was completed, ENF and ELS plates were trimmed and cut into specimens of 190 mm x 20 mm x 6.4 mm and 170 mm x 20 mm x 3 mm, Figure 2. Specimens were then subjected to an edge polishing routine to remove any gross cutting defects along the edges and to enable easier observation of crack onset.

Table 1 - Details of stacking sequence for ENF and ELS shaped and circular fibre specimens.

Mid-plane interface	Stacking sequence (// mid-plane, / in-house, C commercial)
ENF $0^\circ/0^\circ$	$[0_{16C}^o / 0_{8I}^o // 0_{8I}^o / 0_{16C}^o]$
ENF $0^\circ/90^\circ$	$[90_C^o / 0_{2C}^o / 90_C^o / 0_C^o / 90_{2C}^o / 0_C^o / 90_C^o / 0_{2C}^o / 90_C^o / 0_C^o / 90_{2C}^o / 0_C^o / 90_C^o / 0_{2C}^o / 90_C^o // 0_C^o / 90_{2C}^o / 0_C^o / 0_I^o / 90_{2I}^o / 0_I^o / 90_I^o / 0_{2I}^o / 90_I^o // 0_I^o / 90_{2I}^o / 0_I^o / 90_I^o / 0_{2I}^o / 90_I^o / 90_C^o / 0_{2C}^o / 90_C^o / 0_C^o / 90_{2C}^o / 0_C^o / 90_C^o / 0_{2C}^o / 90_C^o / 0_C^o / 90_{2C}^o / 0_C^o]$
ELS $0^\circ/0^\circ$	$[0_{8C}^o / 0_{4I}^o // 0_{4I}^o / 0_{8C}^o]$
ELS $0^\circ/90^\circ$	$[0_C^o / 90_{2C}^o / 0_C^o / 0_C^o / 90_{2C}^o / 0_C^o / 90_I^o / 0_{2I}^o / 90_I^o // 0_I^o / 90_{2I}^o / 0_I^o / 90_C^o / 0_{2C}^o / 90_C^o / 90_C^o / 0_{2C}^o / 90_C^o]$

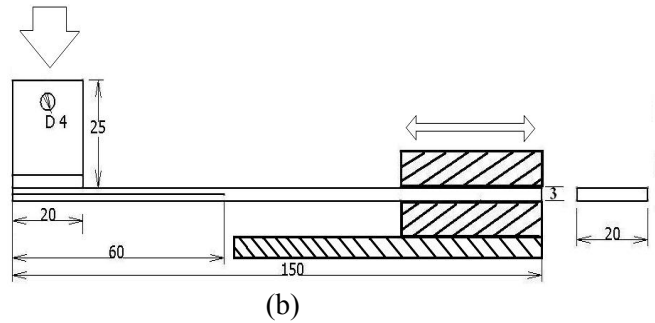
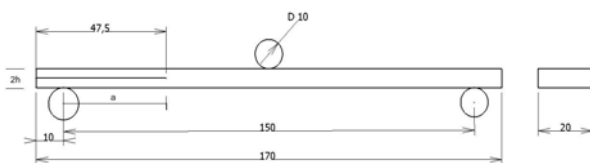


Fig. 2: (a) ENF and (b) ELS specimen and test geometry (in mm).

3 Experimental

3.1 Mode-I pre-cracking

A mode-I opening load was applied to all specimens to propagate the crack beyond the resin rich pocket resulting from the PTFE film crack initiator. Undrilled strap hinges (85 mm x 20 mm x 1.5 mm) were attached to the top and bottom of each specimen with a high peel strength epoxy resin (ARALDITE™ 2021). A thin layer of correction fluid was applied to the longitudinal side face of the specimen, a paper scale attached and a lamp positioned to enhance the visibility of the crack front. Mode-I crack propagation was then carried out using a Hounsfield Electro-mechanical test machine with a 25 kN load cell at a rate of 5.0 mm min⁻¹. Once the crack was sufficiently propagated beyond the resin rich zone, the specimen length was reduced by removal of the strap hinges. The modified ENF and ELS specimen dimensions were in accordance with AECMA standard, Davidson et al [7] and ESIS TC 4 Meeting [34] (Figure 2). Although the AECMA standard [5] and ESIS TC 4 Meeting [34] are only applicable to unidirectional specimens, it was felt that additional information could be obtained by also investigating cross-ply laminates. All laminates were made of commercial E-glass/913 epoxy (ply thickness 0.125, fibre volume fraction 65%, fibre diameter 12 μ m) combined with in-house manufactured borosilicate glass fibre/913 epoxy (ply thickness 0.147 mm, fibre volume fraction approx. 54% and 58% for circular and hollow shaped fibre respectively, Table 2).



(a)

Table 2: Volume fraction analysis of Results of ENF and ELS specimens as determined by resin burn-off.

Specimen type	V_f (%)	V_M (%)	V_v (%)
shaped	57.5	33.8	8.7
circular	53.3	46.0	0.7

The crack is assumed to propagate along the mid-plane interface, thus to ensure evaluation of representative $G_{IIC}(\text{initiation})$ and $G_{IIC}(\text{propagation})$, several plies above and below the mid-plane comprise in-house manufactured material in both circular and shaped fibre laminates. Due to manufacturing constraints, the ENF specimens were 20 mm wide rather than 25 mm as recommended by the AECMA standard [5]. However, a review of mode-II interlaminar fracture toughness [7] confirms the acceptability of this reduced dimension specimen. The ELS specimens were 3 mm thick. Although ESIS TC 4 Meeting [34] suggests a thickness of 5 mm for glass fibre-reinforced specimen, thinner specimens are also admitted as long as the sample widths are maintained between 15 mm and 30 mm.

3.2 Mode-II interlaminar fracture toughness testing

3.2.1 ENF testing

Testing was carried out via three-point bend flexural geometry at a rate of 1 mm min^{-1} under displacement control using a Roell Amsler HTC test machine with a 25 kN load cell controlled by an Instron 8800 controller. Eight replicates were tested for each of the circular and hollow shaped specimen interfaces investigated. Testing was considered as completed when the crack length was equal to half of the span length (75 mm).

3.2.2 ELS testing

Four batches (eight replicates of each interface type) of specimens were end tabbed with aluminium blocks using ARALDITE 2021 and tested using an Instron 4507 screw driven 200KN frame with 1KN load cell at a rate of 1 mm min^{-1} . Experimental data were subjected to a compliance calibration according to ESIS TC 4 Meeting [34]. The associated expression for compliance, C (δ/P),

comes from an experimental curve in which C is plotted against cubed crack length:

$$C = A + ma^3 \quad (1)$$

where A is the initial compliance and m is the gradient.

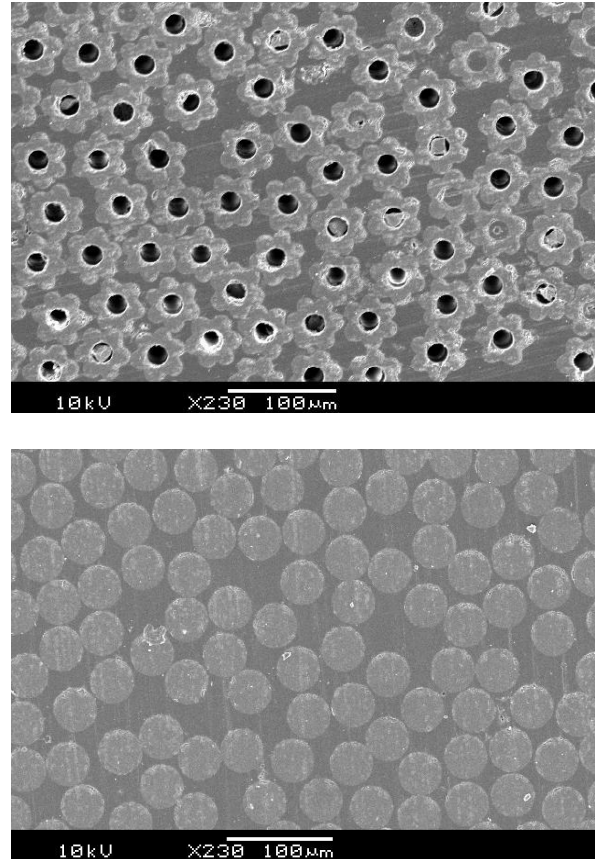


Fig. 3. Through-thickness SEM micrographs showing structure in *SGF* (upper) and *CGF* (above) composites.

4 Results and discussion

Through-the-thickness SEM images (Figure 3) show fibre's misalignment, entrapped air bubbles and voids were minimal in manufactured laminates. Despite great care taken in manufacturing, Table 3 indicates differences in terms of fibre volume fraction (3.7% higher in shaped composites) and overall resin volume fraction (12.2% lower in shaped composites) between laminates reinforced with the two fibre types. The amount of resin is thought to play a key role in mode-II interlaminar fracture toughness of fibrous composites. Singh and Partridge [43] have found that the G_{II} strain energy release rate increases at interfaces with a thicker matrix layer, with specimens containing a resin rich

interface exhibiting up to 200% increase in delamination resistance. In accordance with the differences in fibre and resin volume fractions reported in Table 3, an image analysis approach was used to show that the shaped fibre packing geometry has a mean layer of matrix between neighbouring fibres approximately 50% thinner than for circular fibre packing geometry. Also, the different moment

Table 3: Normalised $G_{IIC(\text{initiation})}$ strain energy release rate for shaped and circular fibre composites

G_{IIC} expression	Specimen type	Norm G_{IIC} (J/m ²)	Exptl. V_f (%)	Exptl. V_M (%)	Av. V_f (%)	Av. V_M (%)
$\frac{9P\delta\alpha^2}{2B(2L^3 + 3a^3)}$	0°/0° shaped	1754	57.5	33.8	55.4	39.9
	0°/0° circular	1414	53.3	46.0	55.4	39.9
CBT3[7]	0°/90° shaped	1374	57.5	33.8	55.4	39.9
	0°/90° circular	1285	53.3	46.0	55.4 </td <td>39.9</td>	39.9

inertia of the two fibre types (22% higher in shaped fibre) is another parameter which will have a direct effect on the stiffness of shaped composites compared to circular. As the derivation of G_{IIC} is strongly related to load/displacement characteristics of the specimen, it is expected that G_{IIC} for a shaped fibre composite could be underestimated when compared to G_{IIC} of a circular composite because of the lower compliance. In an attempt to account for all the above differences between the two composite types, a correction factor f based on the manufacturing parameters (Table 3) was devised. This correction factor was applied to both CBT3 [7] and CC [34] expressions for $G_{IIC(\text{initiation})}$ and $G_{IIC(\text{propagation})}$ respectively, as follows:

$$G_{IIC(\text{normalized})} = G_{IIC} \times f \quad (2)$$

where:

$$f = \left[\frac{\text{Average } V_f}{\text{Exptl } V_f} \frac{\text{Exptl } V_m}{\text{Average } V_m} \right]$$

The experimental results obtained are shown in Table 3 and Figures 4 and 5.

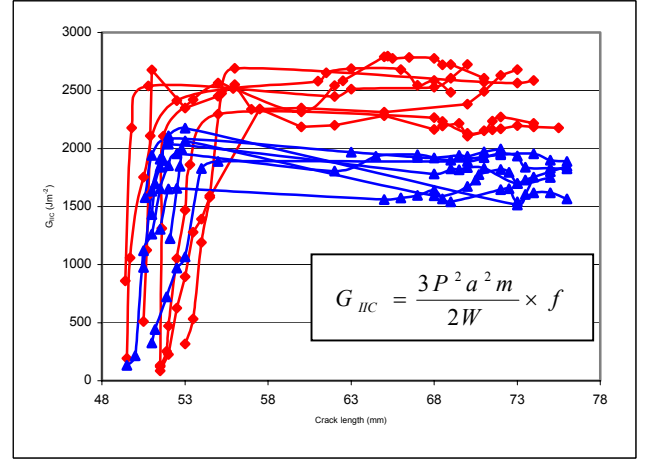


Fig. 4. ELS results for 0°/0° interface, circular fibres (Δ) and shaped fibres(◇)

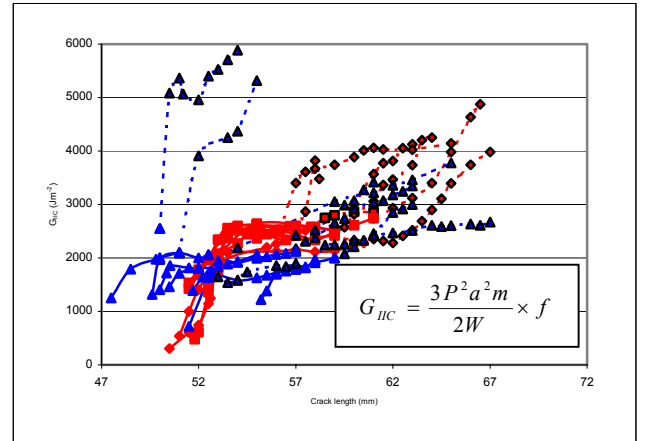


Fig. 5. ELS results for 0°/90° interface, circular fibres (Δ) and shaped fibres(◇). Cross-hatching and black foreground to indicate crack propagating through in-house/commercial or commercial layers only.

4.1 ENF 0°/0° interface.

Initiation strain energy release rate, $G_{IIC(\text{initiation})}$, of shaped fibre laminates was 19% higher than circular laminates. The crack stayed on the 0°/0° interface in both shaped and circular specimens after mode-I delamination growth. SEM micrographs (Figures 6 & 7) show a clearer transition from mode-I to mode-II fracture in circular fibre specimens compared to shaped specimens. In the latter case, the transition between the two fracture modes appears to be more diffuse and occurs over a larger portion of the length. Thus,

the $G_{IIC(\text{initiation})}$ value of shaped fibre specimens was possibly decreased by the previous mode-I damage. Mode-II fracture surface in shaped fibre reinforced laminates shows pronounced hackles (Figures 6) suggesting a stronger interface strength and energy dissipation compared to circular fibre laminates.

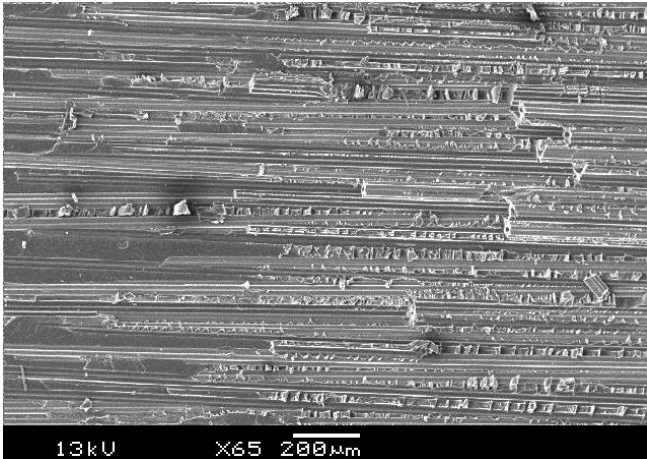


Fig. 6. SEM micrograph showing fractured surface from mode-I (*left*) to mode-II (*right*) in ENF 0°/0° shaped specimen with fibre breakage and more hackles compared to circular.

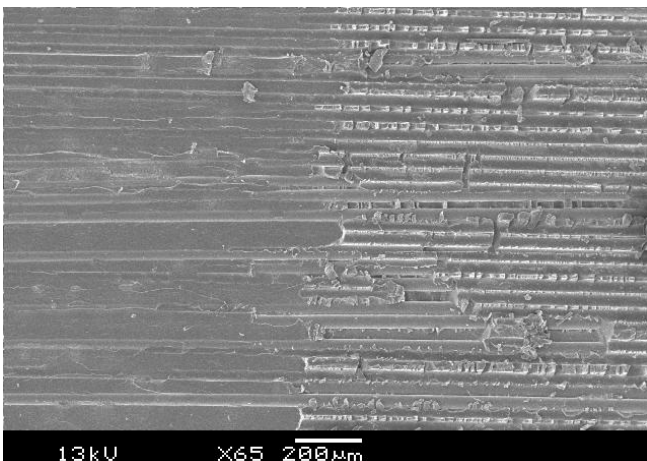


Fig. 7. SEM micrograph showing ENF 0°/0° circular specimen clear passage from mode-I (*left*) to mode-II (*right*) fracture unlike in shaped

4.2 ENF 0°/90° interface.

During mode-I pre-crack loading, the crack has jumped from the 0°/90° mid-plane interface to the upper 90°/0° interface. In mode-II loading condition the crack propagation was both intralaminar and interlaminar in shaped and circular specimens (Figures 8 & 9). On average shaped fibre laminates

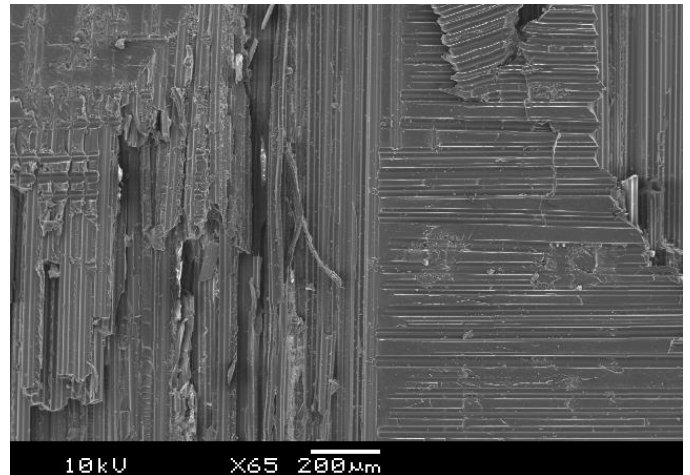


Fig. 8. ENF 0°/90° shaped interface showing intralaminar crack growth both in mode-I (*left*) and mode-II (*right*)

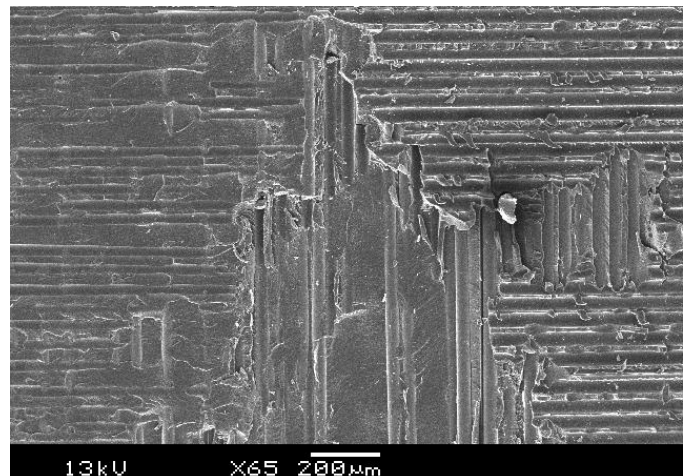


Fig. 9. ENF 0°/90° circular interface showing intralaminar crack growth both in mode-I (*left*) and mode-II (*right*) but not as much as for the shaped fibres

have shown a 6% higher strain energy release rate, $G_{IIC(\text{initiation})}$, compared to circular. This small difference is probably a consequence of the larger portion of intralaminar fracture noted in the shaped specimens. This may be explained in terms of the greater stress concentration associated with the shaped fibres [41]. Conversely, the higher stress concentration at the fibre/matrix interface in shaped composites seems to promote a more stable crack propagation as well as higher damage resistance compared to circular.

4.3 ELS 0°/0° interface.

ELS testing has confirmed the same trend as ENF testing. Figure 4 clearly shows the higher $G_{IIC(\text{propagation})}$, strain energy release rate, for shaped

composite compared to circular. Moreover, shaped fibre specimens have shown more consistent crack initiation as well as more stable propagation. In both cases (shaped and circular) the crack path always propagated through in-house manufactured layers. Crack jumping from the mid-plane interface was rarely observed suggesting the suitability of the selected lay-ups and the specimen geometries (Table 1). SEM analysis (Figures 10 & 11) has shown pronounced hackle markings as well as greater evidence of matrix plastic deformation on shaped fibre fracture surfaces compared to circular despite the lower resin fraction in the former (Table 2).

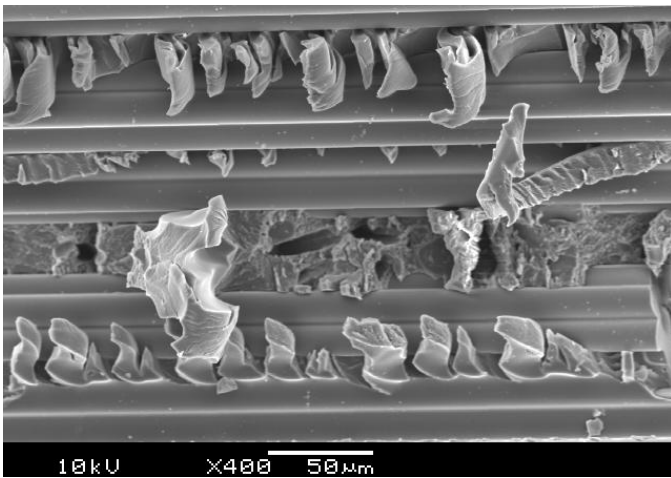


Fig. 10. Mode-II fracture in ELS 0°/0° shaped composite showing marked hackling and matrix toughening effect despite the lower amount of resin compared to circular composite.

4.4 ELS 0°/90° interface.

Circular fibre cross-ply laminates are characterized by much greater specimen deflection during testing compared to corresponding shaped fibre laminates. In these laminates the mode-II crack has propagated through several plies eventually reaching the in-house ply - commercial ply interface (Figures 12 & 13). In the worst case, the crack

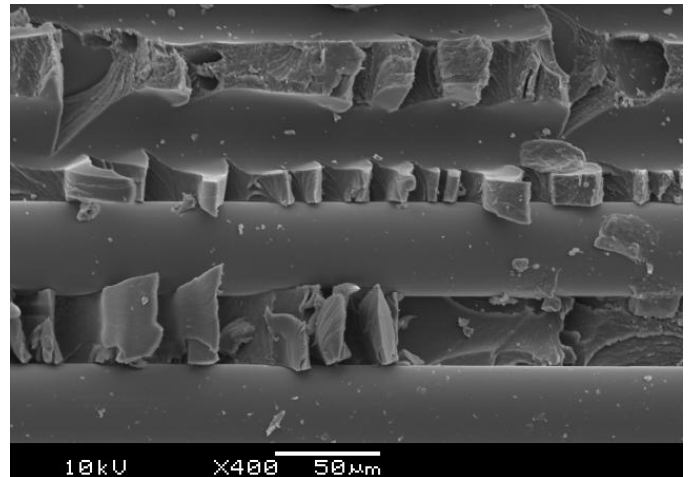


Fig. 11. Mode-II fracture in ELS 0°/0° circular composite showing fewer hackles and general matrix toughening

propagation has passed into commercial ply interfaces within the lower arm of most circular specimens (Figure 13). The high specimen deflection was overcome by reducing the specimen free length with an inevitable loss of propagation values. However, sufficient data were obtained to describe the behaviour of these two composite types. Shaped fibre specimens have shown higher mean $G_{IIC(propagation)}$ compared to circular, but the high scatter observed (Figure 5) brings about some uncertainty.

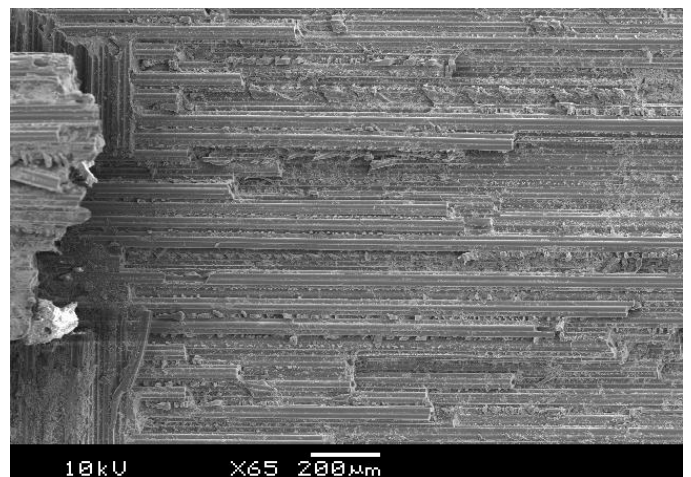


Fig. 12. ELS cross-ply (0°/90°) shaped specimen showing mode-II crack has jumped from the 0°/90° mid-plane interface to the lower layers but staying within in-house plies

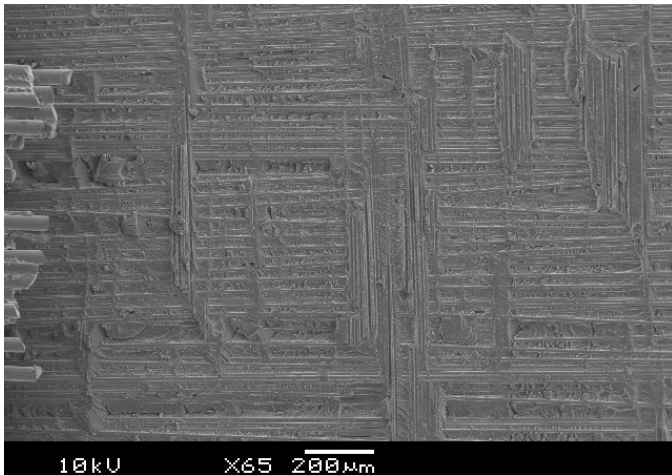


Fig. 13. ELS cross-ply ($0^\circ/90^\circ$) circular specimen showing mode-II crack has jumped from $0^\circ/90^\circ$ mid-plane interface and propagated until intersection with commercial plies.

5 Conclusions

In this investigation, a total of sixty four specimens have been studied using two different mode-II test geometries (ENF and ELS) and two interfaces ($0^\circ/0^\circ$ and $0^\circ/90^\circ$) to evaluate the possible benefit of using shaped fibre reinforcement to improve fracture toughness in FRP composite materials.

A combination of commercial and in-house manufactured pre-impregnated tape types were used successfully (for time saving purposes) to obtain valid G_{IIC} initiation and propagation strain energy release rate data.

Results have shown an increase in both initiation and propagation strain energy release rates (G_{IIC}) in laminates reinforced using shaped fibre compared with those reinforced with circular fibre. Furthermore, despite the higher stress concentrations which operate in cross-ply shaped fibre laminates and which may effect the strain energy release rate, all shaped composites have shown a more stable crack propagation compared to circular composites. Further investigations are needed to better understand the role of the resin volume fraction in composites reinforced with non-circular fibres and to verify the significance of the improvement in cross-ply laminates which has not appeared as clear as in unidirectional shaped laminates.

Acknowledgements

The authors would like to thank the UK Engineering and Physical Sciences Research Council for the financial support of this investigation

under Grant No. GR/T03390) and BAE Systems - Advanced Technology Centre Sowerby for guidance and the use of testing facilities during this work. The authors would also like to thank the University of Bristol, School of Chemistry for the use of Scanning Electron Microscopy facilities.

References

- [1] Ferguson R.F., Hinton M.J. and Hiley M.J., "Determining the through-thickness properties of FRP materials", *Composites Science and Technology*, Vol. 58, pp 1411-1420, 1998.
- [2] Williams J.G., "On the calculation of energy release rates for cracked laminates". *International Journal of Fracture*, Vol. 36, pp 101-119, 1998.
- [3] Brunner A.J., "Experimental aspects of mode-I and mode-II fracture toughness testing of fibre-reinforced polymer-matrix composites". *Computer Methods in Applied Mechanics and Engineering*, Vol. 185, pp 161-172, 2000.
- [4] Yum Y.J. and You H., "Pure mode I, II and mixed mode interlaminar fracture of graphite/epoxy composite materials". *Journal of Reinforced Plastics and Composites*, Vol. 20, No. 2, pp 794-808, 2001.
- [5] AECMA Standard, "Carbon fibre reinforced plastics test method for the determination of interlaminar fracture toughness energy mode II- G_{IIC} ". *European Society of Aerospace Industries*, December 1995.
- [6] Takeba N. and Ogihara S., "Initiation and growth of delamination from the tops of transverse cracks in CFRP cross-ply laminates". *Composites Science and Technology*, Vol. 52, pp 309-318, 1994.
- [7] Davidson B.D. and Sun X., "Geometry and data reduction recommendations for a standardized end notched flexure test of unidirectional composites". *Journal of ASTM International*, Currently in review, Feb 2006.
- [8] Sun X. and Davidson B.D., "A direct energy balance approach for determining energy release rates in three and four point bend end notched flexure tests". *International Journal of Fracture*, Vol. 135, pp 51-72, 2005.
- [9] Blackman B.R.K., Kinloch A.J. and Paraschi M., "The determination of the mode II adhesive fracture resistance, G_{IIC} , of structural adhesive joints: an effective crack length approach". *Engineering Fracture Mechanics*, Vol. 72, pp 877-897, 2005.
- [10] Szekeřenyi A., "Comparison of some data reduction schemes for composite delamination specimens". *Periodica Polytechnica Ser. Mech. Eng.*, Vol. 48, No. 2, pp. 151-161, 2004
- [11] De Moraes A.B., "Analysis of mode II interlaminar fracture of multidirectional laminates". *Composites: Part A*, Vol. 35, pp 51-57, 2004
- [12] Schön J., Nyman T., Blom A. and Ansell H., "Numerical and experimental investigation of a composite ENF specimen". *Engineering Fracture Mechanics*, Vol. 65, pp 405-433, 2000.

MODE-II INTERLAMINAR FRACTURE INVESTIGATION OF NOVEL SHAPED GLASS FIBRE COMPOSITES

- [13] Stevanovic D., Jar P.Y.B., Kalyanasundaram S. and Lowe A., "On crack-initiation conditions for mode I and mode II delamination testing of composite materials". *Composites Science and Technology*, Vol. 60, pp 1879-1887, 2000.
- [14] Wang H. and Vu-Khanh T., "Use of end-loaded-split (ELS) test to study stable fracture behaviour of composites under mode II loading". *Composite Structures*, Vol. 36, pp 71-79, 1996.
- [15] Sun C.T. and Zheng S., "Delamination characteristics of double-cantilever beam and end-notched flexure composite specimens". *Composites Science and Technology*, Vol. 56, pp 451-459, 1996.
- [16] Wang Y. and Williams J.G., "Correction for Mode II fracture toughness specimens of composites materials". *Composites Science and Technology*, Vol. 43, pp 251-256, 1992.
- [17] Wang J. and Qiao P., "Novel beam analysis of end notched flexure specimen for mode-II fracture". *Engineering Fracture Mechanics*, Vol. 71, pp 219-231, 2004.
- [18] Jiménez M.A. and Miravete A., "Application of the finite-element method to predict the onset of delamination growth". *Journal of Composite Materials*, Vol. 38, No. 15, 2004.
- [19] Hashemi S., Kinloch A.J. and Williams J.G., "The effect of geometry, rate and temperature on the mode I, mode II and mixed-mode I/II interlaminar fracture of carbon-fibre/poly(ether-ether ketone) composites". *Journal of Composite Materials*, Vol. 24, 1990.
- [20] Perez C.L. and Davidson B.D., "Evaluation of pre-cracking methods for the end-notched flexure test". *47th AIAA/ASME/ASCE/AHS/ASC Structure, structural Dynamics, and Materials Conference*, Newport, Rhode Island, pp 1-45, May 2006.
- [21] Davidson B.D., Krüger R. and König M., "Effect of stacking sequence on energy release rate distribution in multidirectional DCB and ENF specimens". *Engineering Fracture Mechanics*, Vol. 55, No. 4, pp 557-569, 1996.
- [22] Liu C., Huang Y. and Stout M.G., "Enhanced mode-II fracture toughness of an epoxy resin due to shear banding". *Acta Metallurgica Inc.*, Vol. 46, No. 16, pp 5647-5661, 1998.
- [23] Deng S., Ye L. and Mai Y.W., "Influence of fibre cross-sectional aspect ratio on mechanical properties of glass-fibre/epoxy composites. II- Interlaminar fracture and impact behaviour" *Composite Science and Technology*, Vol. 59, pp 1725-1734, 1999.
- [24] Reeder J.R., "Refinements to the mixed-mode bending test for delamination toughness". *Journal of Composites, Technology and Research*, Vol. 25, No. 4, 2003.
- [25] Kim B.W. and Mayer A.H., "Influence of fibre direction and mixed-mode ratio on delamination fracture toughness of carbon/epoxy laminates". *Composites Science and Technology*, Vol. 63, pp 695-713, 2003.
- [26] Ducept F., Davies P. and Gamby D., "Mixed mode failure criteria for a glass/epoxy composite and an adhesively bonded composite/composite joint". *International Journal of Adhesives*, Vol.20, pp 233-244, 2000.
- [27] Kinloch A.J., Wang Y., Williams J.G. and Yayla P., "The mixed-mode delamination of fibre composite materials". *Composites Science and Technology*, Vol. 47, pp 225-237, 1993.
- [28] Pereira A.B. and De Morais A.B., "Mode I interlaminar fracture of carbon/epoxy multidirectional laminates". *Composites Science and Technology*, Vol. 64, pp 2261-2270, 2004.
- [29] Olsson R., Thesken J.C., Brandt F., Jönsson N. and Nilsson S., "Investigations of delamination criticality and the transferability of growth criteria". *Composite Structures*, Vol. 36, pp 221-247, 1996.
- [30] Yang Z. and Sun C.T., "Interlaminar fracture toughness of a graphite/epoxy multidirectional composite". *Journal of Engineering Materials and Technology*, Vol. 122, 2000.
- [31] Davies P., Moulin C. and Kausch H.H., "Measurement of G_{IC} and G_{IIC} in carbon/ Epoxy composites". *Composites Science and Technology*, Vol. 39, pp 193-205, 1990.
- [32] Harris J., Bond I.P., Weaver P., Wisnom M.R. and Rezaei A., "Measuring strain energy release rate (G_{IC}) in novel fibre shape composites". *Composites Science and Technology*; Vol. 66, pp 1239-1247, 2006.
- [33] Ducept F., Davies P. and Gamby D., "An experimental study to validate tests used to determine mixed mode failure criteria of glass/epoxy composites". *Composites: Part A*, Vol. 28A, pp 719-729, 1997.
- [34] ESIS TC 4, "Determination of the mode-II delamination resistance of unidirectional fiber-reinforced polymer laminates using the end loaded split specimen (ELS)". ESIS TC 4 Meeting, May 12 1995.
- [35] Sela N. and Ishai O., "Interlaminar fracture toughness and toughening of laminated composite materials: A Review". *Composites*, Vol. 20, No. 5, pp 423-435, 1989.
- [36] Dickinson L.C., Farley G.L. and Hinders M.K., "Translaminar Reinforced Composites: A Review". *Journal Of Composites & Technology & Research*; Vol. 21, pp 3-15, 1999.
- [37] Mouritz, A.P., Bannister, M.K., Falzon, P.J. and Leong, K.H., "Review of applications for advanced 3D fibre textile composites". *Composites A*, Vol. 30, No. 12, pp 1445-1461, 1999.
- [38] Mouritz, A.P., Leong, K.H. and Hersberg, I., A "Review of the effect of stitching on in-plane mechanical properties of fibre reinforced polymer composites". *Composites A*, Vol. 28, No. 12, pp 979-991, 1999.

- [39] Garg, A.C. and Mai, Y.W., "Failure mechanisms in toughened epoxy resins - a Review". *Composites Science and Technology*, Vol. 31, pp 179-223, 1988.
- [40] Kim, J.K. and Mai, Y.W., "High strength, high fracture toughness fibre composites with interface control - a Review". *Composites Science and Technology*, Vol. 41, pp 333-378, 1991.
- [41] Cannas A., Bond I., "Improving the through-thickness mechanical properties of composites using hollow shaped fibres". *ECCM 12-European Conference on Composite Materials, Biarritz (France)*, 29 Aug-1 Sept 2006.
- [42] Harris, J., Bond I.P., Weaver, P., and Wisnom, M., "Improving fibre reinforced plastics' through-thickness properties using novel shaped fibres". *Proceeding IMechE: Pt.L - Journal Of Materials: Design And Applications*, Vol. 218, No. L1, pp29-35, 2004.
- [43] Singh S. and Partridge I.K., "Mixed-mode fracture in an interleaved carbon-fibre/epoxy composite". *Composites Science and Technology*; Vol. 55, pp 319-327, 1995.